



ARCHIVIO ISTITUZIONALE  
DELLA RICERCA

Alma Mater Studiorum Università di Bologna  
Archivio istituzionale della ricerca

Constraining Endomorphin-1 by  $\beta,\alpha$ -Hybrid Dipeptide/Heterocycle Scaffolds: Identification of a Novel  $\kappa$ -Opioid Receptor Selective Partial Agonist

This is the final peer-reviewed author's accepted manuscript (postprint) of the following publication:

*Published Version:*

Constraining Endomorphin-1 by  $\beta,\alpha$ -Hybrid Dipeptide/Heterocycle Scaffolds: Identification of a Novel  $\kappa$ -Opioid Receptor Selective Partial Agonist / De Marco, Rossella; Bedini, Andrea; Spampinato, Santi\*; Comellini, Lorenzo; Zhao, Junwei; Artali, Roberto; Gentilucci, Luca. - In: JOURNAL OF MEDICINAL CHEMISTRY. - ISSN 0022-2623. - STAMPA. - 61:13(2018), pp. 5751-5757. [10.1021/acs.jmedchem.8b00296]

This version is available at: <https://hdl.handle.net/11585/666375> since: 2021-02-25

*Published:*

DOI: <http://doi.org/10.1021/acs.jmedchem.8b00296>

*Terms of use:*

Some rights reserved. The terms and conditions for the reuse of this version of the manuscript are specified in the publishing policy. For all terms of use and more information see the publisher's website.

(Article begins on next page)

This item was downloaded from IRIS Università di Bologna (<https://cris.unibo.it/>).  
When citing, please refer to the published version.

This is the final peer-reviewed accepted manuscript of:

Rossella De Marco, Andrea Bedini, Santi Spampinato, Lorenzo Comellini, Junwei Zhao, Roberto Artali, Luca Gentilucci. Constraining Endomorphin-1 by  $\beta,\alpha$ -Hybrid Dipeptide/Heterocycle Scaffolds: Identification of a Novel  $\kappa$ -Opioid Receptor Selective Partial Agonist. J. Med. Chem. 2018, 61, 5751–5757

The final published version is available online at:  
<http://dx.doi.org/10.1021/acs.jmedchem.8b00296>

Rights / License:

The terms and conditions for the reuse of this version of the manuscript are specified in the publishing policy. For all terms of use and more information see the publisher's website.

*This item was downloaded from IRIS Università di Bologna (<https://cris.unibo.it/>)*

***When citing, please refer to the published version.***

# Constraining endomorphin-1 by $\beta,\alpha$ -hybrid dipeptide/heterocycle scaffolds: identification of a novel $\kappa$ -opioid receptor selective partial agonist.

Rossella De Marco,<sup>†,§</sup> Andrea Bedini,<sup>‡,§</sup> Santi Spampinato,<sup>\*,‡</sup> Lorenzo Comellini,<sup>†</sup> Junwei Zhao,<sup>†</sup> Roberto Artali,<sup>¥</sup> and Luca Gentilucci<sup>\*,†</sup>

<sup>†</sup> Department of Chemistry “G. Ciamician”, University of Bologna, Via Selmi 2, 40126-Bologna, Italy

<sup>‡</sup> Department of Pharmacy and Biotechnology, University of Bologna, Via Irnerio 48, 40126-Bologna, Italy.

<sup>¥</sup> Scientia Advice, 20832-Desio, Monza and Brianza, Italy

**KEYWORDS:** endomorphin; peptidomimetic;  $\kappa$ -opioid receptor; molecular docking; partial agonist;  $\alpha,\beta$ -hybrid dipeptide, tail-flick test

**ABSTRACT:** Herein we present the expedient synthesis of endomorphin-1 analogues containing stereoisomeric  $\beta^2$ -homofreidinger lactam-like scaffolds ([Amo<sup>2</sup>]EM), and we discuss opioid receptor (OR) affinity, enzymatic stability, functional activity, *in vivo* antinociceptive effects, and conformational and molecular docking analysis. Hence, H-Tyr-Amo-Trp-PheNH<sub>2</sub> resulted to be a new chemotype of highly stable, selective, partial KOR agonist inducing analgesia, therefore displaying great potential interest as a painkiller possibly with reduced harmful side effects.

## Introduction

The tetrapeptides endomorphine-1, H-Tyr-Pro-Trp-PheNH<sub>2</sub> (EM1), and endomorphine-2, H-Tyr-Pro-Phe-PheNH<sub>2</sub> (EM2), discovered in the mammalian brain by James Zadina in 1997,<sup>1</sup> are endogenous, highly selective  $\mu$ -opioid receptor (MOR) agonists<sup>1,2</sup> which exhibit outstanding antinociception upon icv and its administration, being effective even toward intractable acute and chronic neuropathic pain.<sup>1,3</sup> Despite their tremendous therapeutic potential as painkillers devoid of the undesired side-effects of the opiate alkaloids,<sup>3,4</sup> their clinical use remained unrealistic, due to poor metabolic stability, inability to cross the BBB, and efficient efflux.<sup>3</sup> Consequently, to improve their PK properties, the structure of the EMs has been subjected to a variety of modifications.<sup>5,6,7,8</sup>

Among the most effective manipulations, the introduction of  $\beta$ -variants in place of Pro<sup>2</sup> yielded bioactive EM analogues with improved metabolic stability. Selected examples include the use of pyrrolidine-3-carboxylic acid,<sup>9,10,11,12</sup>  $\beta$ -homoproline,<sup>13,14</sup> nipecotic acid,<sup>15</sup> and cis-2-aminocyclopentane or hexahydroindole-3-carboxylic acid.<sup>16,17,18</sup>

On the other hand, another widely utilized approach consisted in the introduction of local<sup>19,20</sup> or global conformational constraints,<sup>21,22</sup> to control the 3D structure while maintaining the fundamental interactions with the receptors. For instance, a Freidinger lactam-like structure mimicking a constrained Trp-Phe dipeptide was introduced in EM1 (Figure 1), but the resulting peptidomimetic failed to reproduce the desired bioactive conformation.<sup>23</sup> More interestingly, the spiro-Aba-Gly lactam scaffold (Aba: 4-amino-1,2,4,5-tetrahydro-2-benzazepine-

3-one) was shown to induce a  $\beta$ -turn in a MOR-selective, partial agonist mimetic of EM2 (Figure 1).<sup>24</sup>

In this scenario, we figured EM1 analogues including a  $\beta^2$ -residue at position 2, and a Freidinger lactam-like element across the positions 2 and 3, combined into a composite hybrid  $\beta,\alpha$ -dipeptide/heterocycle scaffold (Figure 1). This was made possible by a procedure recently optimized by us, *i.e.* the expedient cyclization of oligopeptide sequences containing isoserine (iSer), by treatment with disuccinimidylcarbonate (DSC) and a catalytic amount of base.

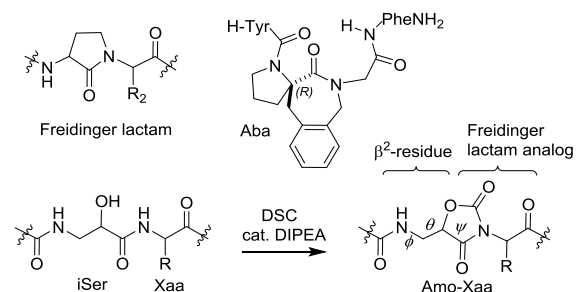


Figure 1. Top: classic Freidinger lactam, and spiro-Aba-Gly lactam; bottom: cyclization of iSer-Xaa to the hybrid  $\beta^2/\alpha$  dipeptide/heterocycle scaffold Amo, with characteristic  $\beta^2$ -residue torsional angles.

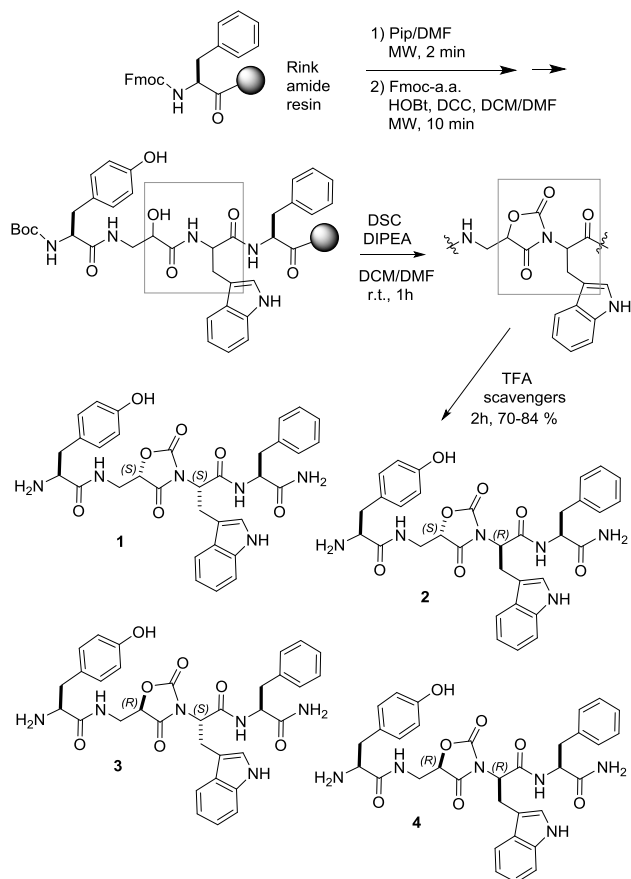
The reaction gave the unprecedented heterocycle 5-(aminomethyl)oxazolidine-2,4-dione (Amo), comprising iSer and the amine group of the following residue Xaa (Scheme 1).<sup>25</sup> This scaffold was successfully exploited to stiffen cyclo-

peptide conformations,<sup>26</sup> and for the preparation of the oxazolidinone antibiotic linezolid in enantiopure form,<sup>27</sup> or enzymatically stable analogues of the  $\alpha 4\beta 1$  integrin antagonist BIO1211.<sup>28</sup>

In this paper we present the synthesis of a mini-library of EM1 analogues containing the central Amo-Trp scaffold in place of Pro<sup>2</sup>-Trp<sup>3</sup> ([Amo<sup>2</sup>]EM), constituted by the four stereoisomers of general sequence H-Tyr-(*S/R*)-Amo-(*S/R*)-Trp-PheNH<sub>2</sub> (Scheme 1), and we discuss their affinity for MOR,  $\delta$ -, and  $\kappa$ -opioid receptors (DOR, and KOR). Subsequently, we analyze the functional activity, the enzymatic stability, and the potential antinociceptive effects of the peptide having the highest receptor affinity. Finally, we investigate the structural determinants for bioactivity by conformational analysis and molecular docking (MDK).

## Results and discussion

**Peptide synthesis.** The [Amo<sup>2</sup>]EMs **1-4** were prepared by solid phase peptide synthesis (SPPS) on a Rink amide resin preloaded with Fmoc-Phe (Scheme 1). Fmoc removal was done with 20% piperidine in DMF at 45°C under microwave irradiation (MW) in 2 min. Fmoc-(*S/R*)-TrpOH, Fmoc-(*S/R*)-iSerOH, Boc-TyrOH, were coupled in sequence using the activating agents DCC and HOBt at 45°C under MW for 10 min.



Scheme 1. SPPS of the diastereoisomeric [Amo<sup>2</sup>]EMs **1-4**.

The resin-bound peptides were treated with 3 equiv. of DSC and 1 equiv. of DIPEA for 1 h. Cleavage from the resin was carried out with TFA and scavengers, at rt for 2 h. The crude peptides were precipitated and collected by centrifuge, and purified by semi-preparative reversed phase (RP) HPLC. The

identity of the [Amo<sup>2</sup>]EM analogues was confirmed by electrospray ionization mass spectrometry (ESI) MS, <sup>1</sup>H NMR, <sup>13</sup>C NMR, and gCOSY spectroscopy; purity was determined by analytical RP HPLC (Table 1), exact mass, and elemental analysis (Supporting Information).

**Human ORs Binding Affinity.** To evaluate any affinity of the [Amo<sup>2</sup>]EMs **1-4** for the ORs, displacement binding assays were performed in HEK-293 cells stably expressing the cloned human (h)MOR, hDOR, or hKOR, using the respective specific radioligands [<sup>3</sup>H]DAMGO, [<sup>3</sup>H]-diprenorphine, or [<sup>3</sup>H]U69,593. The reference compounds DAMGO, DPDPE, and U50,488 showed *K<sub>i</sub>* values in the nM range and high selectivity to the respective receptors (Table 1), as expected. As reported in Table 1, the peptides **2** and **3** did not show any significant receptor affinity. In contrast, H-Tyr-Amo-Trp-PheNH<sub>2</sub> (**1**) displayed a nM affinity for KOR (*K<sub>i</sub>* = 9.8 nM) and high selectivity over MOR and DOR (Table 1). Finally, H-Tyr-(*R*)-Amo-(*R*)-Trp-PheNH<sub>2</sub> (**4**) was a selective MOR ligand, albeit with a modest affinity (*K<sub>i</sub>* = 240 nM) as compared to native EM1 (*K<sub>i</sub>* = 0.36 nM).<sup>1,3</sup>

Table 1. In Vitro OR Affinities of the [Amo<sup>2</sup>]EMs and Reference Compounds for hORs.

compd	Purity (%) <sup>[a]</sup>	<i>K<sub>i</sub></i> (nM) <sup>[b]</sup>		
		MOR	DOR	KOR
DAMGO	-	1.5 ± 0.1	-	-
DPDPE	-	-	3.30 ± 0.05	-
U50,488	-	-	-	2.90 ± 0.04
<b>1</b>	97	>10 <sup>5</sup>	>10 <sup>5</sup>	9.8 ± 4.1
<b>2</b>	95	>10 <sup>5</sup>	>10 <sup>5</sup>	>10 <sup>5</sup>
<b>3</b>	96	>10 <sup>5</sup>	>10 <sup>5</sup>	>10 <sup>5</sup>
<b>4</b>	98	240 ± 50	>10 <sup>5</sup>	>10 <sup>5</sup>

<sup>[a]</sup> Determined by RP-HPLC (General Methods). <sup>[b]</sup> Mean of 4-6 determinations ± SE.

These strikingly different OR preferences suggested that the stereoisomeric Amo-Trp dipeptides induce distinct, alternative 3D geometries to the EM1 analogues. This prompted to investigate the in-solution conformations of **1-4** by NMR spectroscopy and computations (see next sections).

**Stability of **1** and **4** in mouse serum.** The stability of the only bioactive **1** and **4** and of the parent EM1 was determined in mouse serum by RP HPLC and ESI MS analysis, as previously reported.<sup>29</sup> After 1 h, EM1 was almost completely degraded, being present only in traces, as expected on the basis of the literature,<sup>10,13,30</sup> while **1** and **4** were hydrolyzed only to a moderate extent, <5% after 1h, and <10% after 4h, consistent to the peptidomimetic nature of the compounds.<sup>5</sup>

**Pharmacological Characterization of **1** and **4**.** The functional activity of **1** at KOR and of **4** at MOR was investigated by the cAMP test in whole HEK-293 cells stably expressing hKOR (HEK/hKOR) and hMOR (HEK/hMOR), respectively. As expected U50,488 and DAMGO, employed as KOR or MOR reference compounds, significantly inhibited forskolin-induced cAMP accumulation, with IC<sub>50</sub> values of 1.2 nM and 1.5 nM, and *E<sub>max</sub>* of 90% and 95% (*E<sub>max</sub>* = maximal obtainable effect/vehicle), respectively (Table S1). Interestingly, **1** inhibited forskolin-induced cAMP accumulation in HEK/hKOR, with IC<sub>50</sub> = 0.22 nM and *E<sub>max</sub>* = 40%, suggestive of a partial agonist behavior, as compared to U50,488 (IC<sub>50</sub> = 1.2 nM and

$E_{max} = 90\%$ ; Table S1 and Figure 2). Interestingly, when 1  $\mu\text{M}$  **1** was coadministered together with U50,488, 40% inhibition of forskolin-induced cAMP accumulation was observed and U50,488 concentration-response curve was shifted rightward; thus, confirming a partial agonist activity for **1** (Figure 2).

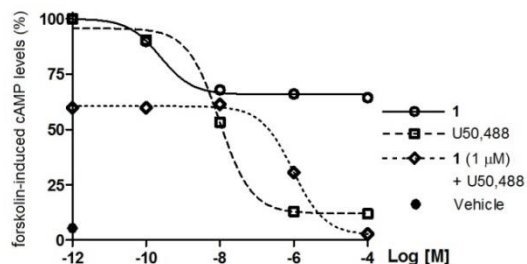


Figure 2. Inhibition of forskolin-induced cAMP accumulation determined by **1** (1 pM - 100  $\mu\text{M}$ ) and U50,488 (1 pM - 100  $\mu\text{M}$ ), alone or co-administered with 1  $\mu\text{M}$  **1**, in HEK/hKOR cells.

On the other hand, **4** inhibited forskolin-induced cAMP accumulation in HEK/hMOR with  $IC_{50} = 0.016$  nM and  $E_{max} = 50\%$  (Table S1), a surprising result when compared to the very modest MOR affinity, in the  $10^{-7}$  M range (Table 1). The partial agonist activity of the [Amo<sup>2</sup>]EMs **1** and **4**, respect to the full agonism of U50,488 and DAMGO, is not completely unexpected. Indeed, the parent peptide EM1 is known to be itself a partial agonist of MOR ( $IC_{50} = 1.0$  nM,  $E_{max} = 53\%$ ) in the cAMP assay,<sup>1,3</sup> and in general its efficacy in many tests is lower than that of synthetic analogues, albeit its antinociceptive efficacy is higher.<sup>1,3</sup>

The tail-immersion test was performed as previously described;<sup>29</sup> the tail of the animal was immersed in hot water and the latency to withdrawal measured in both vehicle- and compound-treated animals. The increase in the latency to response was expressed as MPE% (cutoff 10 s). The curves MPE vs time for ip administered **1** at the dose of 20 mg/kg are shown in Figure 3A.

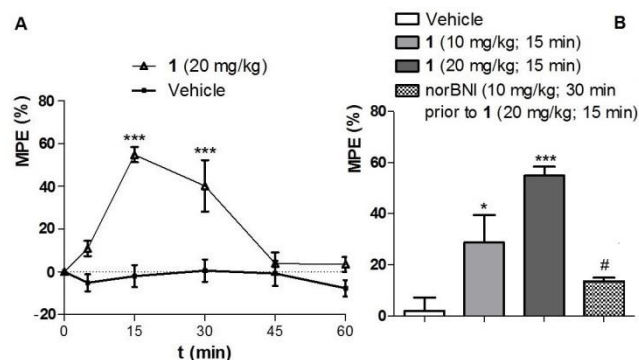


Figure 3. Antinociception produced by **1** in the mouse tail immersion test. **A** Time-dependent effects elicited by ip administered **1** (20 mg/kg); \*\*\*  $p < 0.001$  vs vehicle;  $n = 6$ . **B** Dose-response and KOR-mediated effects induced by ip administered **1** with or without the KOR selective antagonist norBNI; \*  $p < 0.05$  vs vehicle mg/kg; \*\*\*  $p < 0.001$  vs vehicle; #  $p < 0.05$  vs 1 20 mg/kg;  $n = 6$ .

Peptide **1** determined a relevant analgesic effect, which peaked at 15 min (Figure 3A, 60% MPE) and was still significant at 30 min (42% MPE). Interestingly, 10 mg/kg of **1** induced a significant analgesia (15 min), albeit lower as compared to the 20 mg/kg dose (Figure 3B). Antinociceptive effects elicited by

**1** (20 mg/kg, 15 min) were counteracted by the preemptive administration of the KOR selective antagonist nor-BNI (10 mg/kg, 30 min prior to **1**), thus confirming also *in vivo* a KOR-mediated activity (Figure 3B).

The unprecedented pharmacological profile of **1** is of some interest, since this compound represents the first close analogue of EM1 showing nM KOR affinity, partial agonist behavior, high enzymatic stability, and *in-vivo* activity. While the endogenous ligands of KOR, *i.e.* the full agonist dynorphin A (dynA) and truncated sequences, show moderate preference for KOR over DOR and MOR,<sup>31,32</sup> **1** is completely KOR-selective. Among the opiates, KOR agonists and partial agonists have become the object of much interest as painkillers, due to the intrinsic drawbacks of MOR and DOR agonists.<sup>4</sup> Indeed, the former are regarded as the most potent analgesics, but they are accompanied by relevant side-effects, including constipation, respiratory depression, addiction; the latter have a reduced addictive potential, but possess lower antinociceptive effect.<sup>4</sup> KOR is different from the other ORs in terms of tissue expression, functional properties, and side effect profile upon activation. Hence, KOR agonists may produce analgesia without the unwanted effects associated to MOR or DOR,<sup>33</sup> but may induce hallucinations and dysphoria.<sup>4,31</sup> However, KOR partial agonists may allow an analgesic response to be produced at dosages lower than those required to produce the adverse effects.<sup>34</sup> Besides, some KOR agonists display anti-inflammatory and neuroprotective effects, and they suppress the rewarding effects of opiates and cocaine. Partial agonists may hold potential for the treatment of depression, mood disorders,<sup>35</sup> psychiatric co-morbidity, specific drug addictions.<sup>32</sup> Such compounds may restore homeostatic control of dopaminergic function underlying mood and reward. KOR partial agonism may also diminish severity of relapse/re-escalation. Mixed agonists/partial agonists/antagonists at different OR subtypes are employed to treat alcohol dependence and cocaine craving.<sup>4,34,36</sup> As for KOR antagonists, these are already used to treat opioid dependence and withdrawal.<sup>4,37,38</sup>

Interestingly, the [Amo<sup>2</sup>]EM **1** is able to selectively bind to and activate KOR with high affinity, in contrast to the parent EM1, which is a very poor KOR ligand ( $K_i = 5430$  nM),<sup>1,3</sup> albeit they share the same pharmacophores and the same all-*S* stereochemistry pattern. This consideration roused a question, whether the specific doubly (*S*)-configured Amo<sup>2</sup>-Trp<sup>3</sup> central scaffold in **1** might represent a KOR-specific recognition element, or rather it could stabilize a specific bioactive conformation. To address this issue, we analyzed conformations of **1-4** in solution, and we applied MDK computations to gain structural insight into the binding mode to KOR.

**Conformational analysis in-solution.** NMR analysis of **1-4** was performed in 8:2 [D6]dimethylsulfoxide (DMSO)/H<sub>2</sub>O, a solvent mixture often utilized as excellent representative of biological environment for the analysis of opioid peptides.<sup>39,40</sup> The occurrence of hydrogen (H)-bonded structures was excluded on the basis of variable temp NMR experiments. Indeed, the  $\Delta\delta/\Delta t$  parameters of **1-4** suggested that all amide protons were solvent-exposed ( $|\Delta\delta/\Delta t|$  in the 4.5-6.5 p.p.b.  $K^{-1}$  range, not shown). The compounds were analyzed by 2D ROESY, and cross-peaks intensities were utilized to infer constraints for restrained MD simulations (Supporting Information). MD were conducted in a box of explicit water at high temp with scaled restraints, followed by a simulation with full restraints.

After gradually cooling, the structures were minimized with AMBER force field and clustered by the rmsd analysis of the backbone atoms. For all compounds, this procedure gave one major cluster comprising the large majority of the structures. The representative structures with the lowest energy and the least number of restraint violations were selected and analyzed (Figure 4).

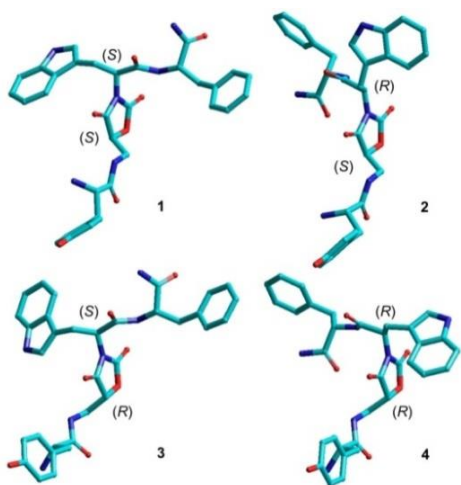


Figure 4. Representative conformers of [Amo<sup>2</sup>]EMs **1-4**, determined by ROESY and restrained MD.

These structures display partially bent backbones; the central dihedral angle Amo $\theta$  (Figure 4) is +g in **1** and **2**, -g in **3** and **4**. For **1** and **4**, Tyr and PheNH<sub>2</sub> lie on the same side of the central homochiral (S,S) and (R,R) Amo-Trp scaffolds. In contrast, for **2** and **3**, which include heterochiral (S,R) or (R,S) scaffolds, the ROESY derived structures reveal more extended backbone conformations, with Tyr on the opposite side respect PheNH<sub>2</sub>.

Starting from these geometries, the dynamic behavior of the peptides was observed by unrestrained MD simulations in explicit water, at rt. During the simulations, the rotation of the backbones around the Amo-Trp bond was not observed, possibly due to the presence of the two carbonyl groups at the positions 2 and 4 of the heterocycle.

**Molecular docking (MDK).** The in-solution structures of **1-4** (Figure 4) were docked with Autodock within a receptor model built from an X-ray structure of the active conformation of KOR in complex with MP1104.<sup>41</sup> All MDK poses were visually inspected for close intermolecular interactions of the binding residues. The pose of peptide **1** with the best score is shown in Figure 5. This complex shows a tight fit of the ligand in the binding cleft, forming ionic, polar, and extensive hydrophobic interactions with the receptor. The plausible “message” portion Tyr<sup>1</sup> of **1** adopts a disposition alternative to that of tetrahydroisoquinoline ring of JD<sub>Tic</sub>,<sup>42</sup> and to the docked pose of the Tyr of the KOR peptide ligand dynA(1-8),<sup>43,44</sup> and finally to the tyramine portion of MP1104,<sup>41</sup> while showing little in common with the binding pose of the conorphins.<sup>45</sup> On the other hand, the rest of the structure of **1** adopts a peculiar, unique orientation within the receptor (Figure 5), occupying an “address-recognition” region which is not conserved across the other ORs.<sup>42,43,46</sup>

This geometry is rather different from that observed in solu-

tion (Figure 4 and Supporting Information), in that Amo ring adopts a *trans* conformation about the  $\theta$  angle, and the Trp-PheNH<sub>2</sub> portion is rotated opposite respect to in-solution **1**. Modeling of KOR revealed that the binding pocket for “address” portion of the ligands is narrowed respect to the other ORs, mostly due to differences in the extracellular loop (EL) 2 and the extracellular parts of the transmembrane helix (TM) 6, and TM7.<sup>42,43</sup> As a consequence, the ligand may be forced to assume a higher energy conformation for optimal fit.<sup>46</sup>

In details, the Tyr of **1** is positioned into the pocket circumscribed by TM3-7 (Figure 5), with the protonated amine forming an hydrogen bond and a ionic interaction (1.5 and 1.2 Å) with the carbonyl and the carboxylate of Asp<sup>138</sup> (3:32 in the Ballesteros and Weinstein numbering system), a residue conserved in all aminergic GPCRs, thereby playing a critical role in binding and activation. The backbone oxygen forms an H-bond (3.0 Å) with the phenolic OH group of Tyr<sup>139</sup> (3:33), a residue postulated to be related to receptor function, while the phenolic OH interacts with the backbone oxygen of Ile<sup>316</sup> (7:39) and the nitrogen of Gly<sup>319</sup> (7:42) forming two H-bonds (1.5 and 2.3 Å, respectively). The phenol group is also stabilized by a favorable  $\pi$ - $\pi$  stacking interaction with the aromatic side chains of Tyr<sup>320</sup> (7:43). It is worth noting that Tyr phenol group holds Trp<sup>287</sup> (6:48), a residue thought to be a key part of the activation mechanism of the receptor, in the rotamer observed in the active-state crystal structure.

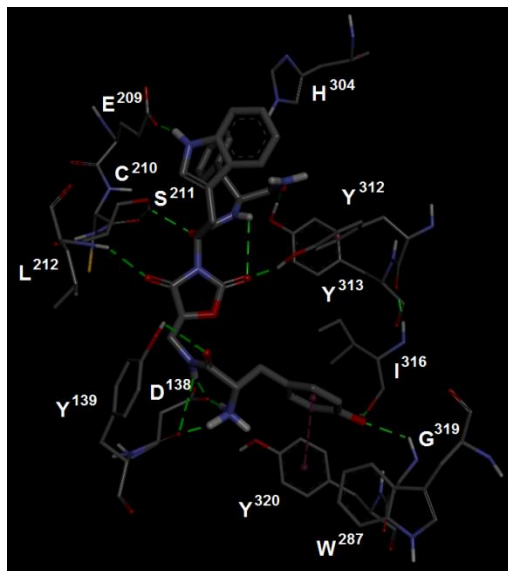


Figure 5. Stabilizing interaction within the complex KOR (PDB ID: 6B73)-**1** represented as dashed lines: H-bonds in green, salt bridges in orange, and  $\pi$ - $\pi$  interactions in violet. KOR residues are rendered in line, while **1** is rendered in stick.

The Amo residue is inserted between TM3, TM6, and TM7, and contributes to the stability of the complex with several H-bonds: two H-bonds between AmoNH and the carboxylate and carbonyl groups of Asp<sup>138</sup> (3:32) (1.7 and 2.9 Å); the C=O in **4** interact with NH of Leu<sup>212</sup> (EL2, 2.4 Å); C=O in **2** forms an H-bond to the phenolic OH of Tyr<sup>312</sup> (7:35, 1.5Å), a residue deeply involved in receptor activation. The latter interaction might contribute to the KOR selectivity of **1**, being such an interaction with a residue in the binding pocket that differ in other closely related ORs (residue 7:35 is Trp in MOR, Leu in DOR).<sup>43</sup>

Trp<sup>3</sup> of **1** resides between TM4-7 and EL2, forming H-bonds between indoleNH and the carboxylate side chain of Glu<sup>209</sup> (EL2, 1.7 Å), and between the backbone carbonyl oxygen and OH of Ser<sup>211</sup> (EL2, 2.7 Å). The indole is also stabilized by a  $\pi$ - $\pi$  stacking interaction with the charged side chain of Lys<sup>227</sup> (5:39). Finally, the C-terminal PheNH<sub>2</sub> of **1** is located between EL2, TM6, and TM7, with carbonyl group forming an H-bond to the phenolic OH of Tyr<sup>313</sup> (7:36, 1.6 Å), and is placed in position also by an intramolecular H-bond between PheNH and Amoco at position 2 (2.9 Å).

As for the other Amo-peptides 2-4, the same MDK protocol as described above failed to furnish high-scoring, representative bioactive geometries in KOR, supporting the fundamental role of the specific stereochemistry of the Amo-Trp scaffold of **1** in orienting the pharmacophores for optimal receptor-specific interactions.

## Conclusions

Aiming at improving stability and bioavailability, the sequence of EM1 was modified by the introduction of the stereoisomeric Amo-Trp hybrid scaffolds, which combine a  $\beta^2$ -homo residue and a Friedinger lactam-like structure. Compound H-Tyr-(R)-Amo-(R)-Trp-PheNH<sub>2</sub> (**4**) maintained the MOR preference of the parent peptide, albeit with strongly reduced affinity. More intriguingly, H-Tyr-Amo-Trp-PheNH<sub>2</sub> (**1**) demonstrated high KOR affinity and selectivity, acting as a partial agonist *in vitro* and determining a relevant analgesia *in vivo* in the tail-immersion test. The clinical utility of opioid analgesics with partial efficacy has been well-documented.<sup>34</sup> Besides, such compounds are currently thought to be a potential strategy in the treatment of psychiatric comorbidity, mood disorders,<sup>35</sup> and specific addictive diseases. Selective KOR partial agonists may be beneficial in promoting more prolonged abstinence, as well as decreasing the severity of relapse episodes.<sup>32</sup> Unfortunately, owing to lack of KOR>MOR selectivity in known ligands, these therapeutic opportunities have been not clinically exploited, so far.<sup>32,33</sup> Molecular modeling and docking analysis shed light on the bioactive structure of this unprecedented chemotype<sup>43</sup> of KOR ligand. The computations support the role of Amo in orienting the pharmacophores for optimal receptor fitting. Besides to the C-terminal Trp<sup>3</sup>-Phe<sup>4</sup>NH<sub>2</sub> portion, Amo<sup>2</sup> itself appear to belong to the “address” of the ligand, being responsible of interactions with residues which are not conserved across the other ORs.

## Experimental section

**General Methods.** Disposables, cells, and any reagents, were obtained from commercial sources. MW heating was performed at 40 W, under automatic temp control. Analytical RP HPLC was carried out on a C18 column (100 × 3 mm, particle size 3  $\mu$ m, pore size 110 Å); DAD 210/246 nm, mobile phase from 9:1 H<sub>2</sub>O/CH<sub>3</sub>CN/0.1% TFA to 2:8 H<sub>2</sub>O/CH<sub>3</sub>CN/0.1% TFA in 20 min, flow rate 0.5 mL min<sup>-1</sup>. Semi-preparative RP HPLC was carried out on a C18 column (150 × 21.2 mm, particle size 7  $\mu$ m, pore size 80 Å), mobile phase from 2:8 H<sub>2</sub>O/CH<sub>3</sub>CN/0.1% TFA to 100% CH<sub>3</sub>CN/0.1% TFA, in 10 min, flow rate 12 mL min<sup>-1</sup>. ESI analysis was carried out using a MS single quadrupole detector. Exact mass was determined on a QTOF apparatus. Elemental analyses utilized a CHNS/O analyzer. <sup>1</sup>H NMR spectra were registered at 400 MHz in 8:2 DMSO-d<sub>6</sub>/H<sub>2</sub>O (water presaturation), and <sup>13</sup>C NMR spectra at 100 MHz. Purity was determined to be  $\geq$ 95%

by analytical RP HPLC, exact mass, and elemental analysis; all details are given in the Supporting Information.

**SPPS.** The linear peptides were assembled on a Fmoc-Phe-preloaded (0.2-0.6 mmol/g) Rink amide resin. Fmoc was removed with 1:4 piperidine/DMF at 45°C under MW irradiation, in 2 min. Fmoc-amino acids (0.6 mmol) were coupled in sequence using DCC/HOBt (0.6/0.6 mmol) in DMF at 45°C under MW, in 10 min. Full details are given in the Supporting Information. To obtain the Amo ring, the iSer-containing peptidyl resins were suspended in 4:1 CH<sub>2</sub>Cl<sub>2</sub>/DMF, and treated with DSC (3 equiv) and DIPEA (3 equiv) for 1h.

**Peptide cleavage.** The Amo-containing peptidyl resins were cleaved with 7:1:1:1 TFA/triisopropylsilane/water/PhOH for 2 h at rt. The crude peptides were precipitated from ice cold Et<sub>2</sub>O (69-84% pure by RP HPLC), and isolated by semipreparative RP HPLC (purity 95-98 %).

**OR affinities.** Displacement binding assays were performed in HEK-293 cells stably expressing the hMORs, using the radioligands [<sup>3</sup>H]DAMGO, [<sup>3</sup>H]-diprenorphine, and [<sup>3</sup>H]U69,593, to label MOR, DOR, or KOR, respectively. In brief, compounds were incubated at 25°C for 120 min in Tris-HCl buffer and 0.3% BSA on cell membranes in the concentration range 10<sup>-12</sup>-10<sup>-4</sup> M; nonspecific binding was determined in the presence of the cold ligands. Cells lysed with 0.1 N NaOH were left in scintillation fluid for 8 h before counting. The radioactivity trapped on filters presoaked with 0.3% polyethylenimine was determined by liquid scintillation. K<sub>i</sub> values were calculated using the Cheng-Prusoff equation from the IC<sub>50</sub>. Full details are given in the Supporting Information.

**Enzymatic stability.** The stability of **1**, **4**, and EM1, in mouse serum, was determined during a 4 h incubation at 37°C. The mixture were successively sampled, and enzymatic activity was terminated with glacial acetonitrile. After centrifuge, the supernatants were collected and the amount of intact peptides was determined by RP HPLC. More details are given in the Supporting Information.

**cAMP functional assay.** The agonist activity of **4** and **1** was determined by measuring the inhibition of forskolin-stimulated cAMP accumulation in whole HEK-293 cells expressing MOR and KOR, respectively. Cells were incubated in serum-free medium containing 0.5 mM 3-isobutyl-1-methylxanthine and exposed for 15 min to 10  $\mu$ M forskolin without and with the compounds at conc from 1 to 100  $\mu$ M, at 37°C. To better characterize partial agonism of **1**, HEK/hKOR cells were exposed to U50,488 at conc from 1pM to 100  $\mu$ M with or without 1  $\mu$ M **1**. cAMP concentration was determined using a cAMP EIA kit. See also the Supporting Information.

**Warm-water tail-immersion test.**<sup>29</sup> Briefly, a mouse's tail was immersed in hot water (52  $\pm$  0.5 °C). Prior to being treated, each mouse was tested to record control latency to withdrawal (CL). Animals responding within 5 s were then ip injected with either vehicle or **1** (10 or 20 mg/kg), with or without norBNI (10 mg/kg; 30 min prior than **1**), and test latency (TL) was determined (cutoff 10 s). The antinociceptive response was expressed as MPE% = 100 × (TL - CL)/(10 - CL).

**Conformational Analysis.** 2D ROESY experiments were performed in DMSO-d<sub>6</sub>/H<sub>2</sub>O (8:2). Cross-peak intensities were classified as very strong, strong, medium, and weak and were associated with distances of 2.3, 2.7, 3.3, and 5.0 Å, respec-

tively, utilized as constraints in the MD simulations. For the absence of  $\text{Ha}(i)\text{-Ha}(i+1)$  cross-peaks, the  $\omega$  bonds were set at  $180^\circ$ . The restrained MD was conducted using the AMBER force field in a  $30 \text{ \AA}^3$  box of TIP3P models of equilibrated water. Random structures were subjected to a 50 ps restrained MD with a 50% scaled force field at 1200 K, followed by 50 ps with full restraints, after which the system was cooled in 20 ps to 50 K. The resulting structures were minimized, and backbones were clustered by the rmsd analysis. Unrestrained MD simulations were conducted for 10 ns at 298 K using periodic boundary conditions (see also the Supporting Information).

**Molecular docking (MDK) for 1 and hKOR (PDB ID: 6B73).** Computations were performed with Autodock 4.0, using the Lamarckian Genetic Algorithm. Ligands and receptors were further processed using the Autodock Tool Kit. 250 independent docking runs were carried out (Autogrid), the results were scored with the Weiner force field, and clustered by rmsd. Residues within  $5.0 \text{ \AA}$  from the center of the binding site were allowed to be flexible. Energy minimizations were performed with the CUDA® version of GROMACS and the AMBER-03 force field. MD simulations were performed at 300 K and 1 bar, in a cube of TIP3P water molecules. Final simulations were carried out under V-rescale temp and Parrinello-Rahman pressure coupling algorithms. The particle-mesh Ewald algorithm was utilized to calculate long-range electrostatics, while Linear Constraint Solver method was used to constrain all covalent bond lengths (more details in Supporting Information).

## ASSOCIATED CONTENT

**Supporting Information.** The Supporting Information is available free of charge on the ACS Publications website at DOI: xxxxx. Full experimental details, ROESY cross peaks, Molecular formula strings and some data (CSV)

## AUTHOR INFORMATION

### Corresponding Author

\*L.G.: e-mail: luca.gentilucci@unibo.it; phone: +39 0512099570; fax: +39 0512099456; Web: <http://www.ciam.unibo.it/gentilucci>

S.S.: e-mail: santi.spampinato@unibo.it; phone, +39 0512091797; fax: +39 051 2091780; Web: <https://www.unibo.it/sitoweb/santi.spampinato>

### Author Contributions

§ These authors contributed equally.

## ACKNOWLEDGMENT

WE thank University of Bologna, FARB (FFBO 125290), Fondazione Veronesi-Milano (Proj. Tryptoids) for financial support.

## ABBREVIATIONS

MOR, DOR, KOR,  $\mu$ -,  $\delta$ -,  $\kappa$ -opioid receptor; Amo, 5-(aminomethyl)oxazolidine-2,4-dione; MW, microwave; DIPEA, diisopropylethylamine; HOBt, hydroxybenzotriazole; DCC, N,N'-dicyclohexylcarbodiimide; RP, reversed phase; SEM, standard error of the mean; MDK, molecular docking; rmsd, root-mean-square deviation

## REFERENCES

- (1) Zadina, J. E.; Hackler, L.; Ge, L. J.; Kastin, A. J. A potent and selective endogenous agonist for the mu-opiate receptor. *Nature*, **1997**, *386*, 499-502.
- (2) Harrison, C.; McNulty, S.; Smart, D.; Rowbotham, D. J.; Grandy, D. K.; Devi, L. A.; Lambert, D. G. The effects of endomorphin-1 and endomorphin-2 in CHO cells expressing recombinant mu-opioid receptors and SH-SY5Y cells. *Br. J. Pharmacol.* **1999**, *128*, 472-478.
- (3) Fichna, J.; Janecka, A.; Costentin, J.; Do Rego, J. C. The endomorphin system and its evolving neurophysiological role. *Pharmacol. Rev.* **2007**, *59*, 88-123.
- (4) Aldrich, J. V.; McLaughlin, J. P. Opioid Peptides: Potential for drug development. *Drug Discov. Today Technol.* **2012**, *9*, e23-e31.
- (5) Keresztes, A.; Borics, A.; Tóth, G. Recent advances in endomorphin engineering. *Chem. Med. Chem.* **2010**, *5*, 1176-1196.
- (6) De Marco, R.; Janecka, A. Strategies to improve bioavailability and in vivo efficacy of the endogenous opioid peptides endomorphin-1 and endomorphin-2. *Curr. Top. Med. Chem.* **2015**, *16*, 141-155
- (7) Varamini, P.; Tóth, I. Lipid- and sugar-modified endomorphins: novel targets for the treatment of neuropathic pain. *Front. Pharmacol.* **2013**, *4*, 1-7.
- (8) Liu, W. X.; Wang, R. Endomorphins: potential roles and therapeutic indications in the development of opioid peptide analgesic drugs. *Med. Res. Rev.* **2012**, *32*, 536-580.
- (9) Cardillo, G.; Gentilucci, L.; Melchiorre, P.; Spampinato, S. Synthesis and binding activity of endomorphin-1 analogues containing beta-amino acids. *Bioorg. Med. Chem. Lett.* **2000**, *10*, 2755-2758.
- (10) Cardillo, G.; Gentilucci, L.; Tolomelli, A.; Calienni, M.; Qasem, A. R.; Spampinato, S. Stability against enzymatic hydrolysis of endomorphin-1 analogues containing beta-proline. *Org. Biomol. Chem.* **2003**, *1*, 1498-1502.
- (11) Liu, X.; Wang, Y.; Xing, Y.; Yu, J.; Ji, H.; Kai, M.; Wang, Z.; Wang, D.; Zhang, Y.; Zhao, D.; Wang, R. Design, synthesis, and pharmacological characterization of novel endomorphin-1 analogues as extremely potent  $\mu$ -opioid agonists. *J. Med. Chem.* **2013**, *56*, 3102-3114.
- (12) Perlikowska, R.; Pieknielna, J.; Mazur, M.; Koralewski R.; Olczak, J.; do Rego, J. C.; Fichna, J.; Modranka, J.; Janecki, T.; Janecka, A. Antinociceptive and antidepressant-like action of endomorphin-2 analogs with proline surrogates in position 2. *Bioorg. Med. Chem.* **2014**, *22*, 4803-4809.
- (13) Cardillo, G.; Gentilucci, L.; Qasem, A. R.; Sgarzi, F.; Spampinato, S. Endomorphin-1 analogues containing beta-proline are mu-opioid receptor agonists and display enhanced enzymatic hydrolysis resistance. *J. Med. Chem.* **2002**, *45*, 2571-2578.
- (14) Spampinato, S.; Qasem, A. R.; Calienni, M.; Murari, G.; Gentilucci, L.; Tolomelli, A.; Cardillo, G. Antinociception by a peripherally administered novel endomorphin-1 analogue containing beta-proline. *Eur. J. Pharmacol.* **2003**, *469*, 89-95.
- (15) Perlikowska, R.; Gach, K.; Fichna, J.; Tóth, G.; Walkowiak, B.; do-Rego, J. C.; Janecka, A. Biological activity of endomorphin and [Dmt1]endomorphin analogs with six-membered proline surrogates in position 2. *Bioorg. Med. Chem.* **2009**, *17*, 3789-3794.
- (16) Keresztes, A.; Szucs, M.; Borics, A.; Kövér, K. E.; Forró, E.; Fülöp, F.; Tömböly, C.; Péter, A.; Páhi, A.; Fábíán, G.; Murányi, M.; Tóth, G. New endomorphin analogues containing alicyclic beta-amino acids: influence on bioactive conformation and pharmacological profile. *J. Med. Chem.* **2008**, *51*, 4270-4279.
- (17) Borics, A.; Mallareddy, J. R.; Timári, I.; Kövér, K. E.; Keresztes, A.; Tóth, G. The effect of Pro(2) modifications on the structural and pharmacological properties of endomorphin-2. *J. Med. Chem.* **2012**, *55*, 8418-8428.
- (18) Mallareddy, J. R.; Borics, A.; Keresztes, A.; Kövér, K. E.; Tourwé, D.; Tóth, G. Design, synthesis, pharmacological evaluation, and structure-activity study of novel endomorphin analogues with multiple structural modifications. *J. Med. Chem.* **2011**, *54*, 1462-



1472.

(19) Harrison, B. A.; Gierasch, T. M.; Neilan, C.; Pasternak, G. W.; Verdine, G. L. High-affinity mu opioid receptor ligands discovered by the screening of an exhaustively stereodiversified library of 1,5-enediols. *J. Am. Chem. Soc.* **2002**, *124*, 13352-13353.

(20) Keller, M.; Boissard, C.; Patiny, L.; Chung, N. N.; Lemieux, C.; Mutter, M.; Schiller, P. W. Pseudoproline-containing analogues of morphiceptin and endomorphin-2: evidence for a cis Tyr-Pro amide bond in the bioactive conformation. *J. Med. Chem.* **2001**, *44*, 3896-3903.

(21) Cardillo, G.; Gentilucci, L.; Tolomelli, A.; Spinosa, R.; Calinenni, M.; Qasem, A. R.; Spampinato S. Synthesis and evaluation of the affinity toward mu-opioid receptors of atypical, lipophilic ligands based on the sequence c[-Tyr-Pro-Trp-Phe-Gly-]. *J. Med. Chem.* **2004**, *47*, 5198-5203.

(22) Perlikowska, R.; Pieknielna, J.; Gentilucci, L.; De Marco, R.; Cerlesi, M. C.; Calo, G.; Artali, R.; Tömböly, C.; Kluczyk, A.; Janecka, A. Synthesis of mixed MOR/KOR efficacious cyclic opioid peptide analogs with antinociceptive activity after systemic administration. *Eur. J. Med. Chem.* **2016**, *109*, 276-286.

(23) Pulka, K.; Feytens, D.; Van den Eynde, I.; De Wachter, R.; Kosson, P.; Misicka, A.; Lipkowski, A.; Chung, N. N.; Schiller, P. W.; Tourwé, D. Synthesis of 4-amino-3-oxo-tetrahydroazepino[3,4-b]indoles: new conformationally constrained Trp analogs. *Tetrahedron* **2007**, *63*, 1459-1466.

(24) Tömböly, C.; Ballet, S.; Feytens, D.; Kövér, K. E.; Borics, A.; Lovas, S.; Al-Khrasani, M.; Fürst, Z.; Tóth, G.; Benyhe, S.; Tourwé, D. Endomorphin-2 with a beta-turn backbone constraint retains the potent mu-opioid receptor agonist properties. *J. Med. Chem.* **2008**, *51*, 173-177.

(25) Greco, A.; Tani, S.; De Marco, R.; Gentilucci, L. Synthesis and analysis of the conformational preferences of 5-aminomethylloxazolidine-2,4-dione scaffolds: first examples of  $\beta^2$ - and  $\beta^{2,2}$ -homo-Freidinger lactam analogues. *Chem. Eur. J.* **2014**, *20*, 13390-13404.

(26) Gentilucci, L.; Gallo, F.; Meloni, F.; Mastandrea, M.; Del Secco, B.; De Marco, R. Controlling cyclopeptide backbone conformation with  $\beta/\alpha$ -hybrid peptide-heterocycle scaffolds. *Eur. J. Org. Chem.* **2016**, 3243-3251

(27) Greco, A.; De Marco, R.; Tani, S.; Giacomini, D.; Galletti, P.; Tolomelli, A.; Juaristi, E.; Gentilucci, L. Controlling cyclopeptide backbone conformation with  $\beta/\alpha$ -hybrid peptide-heterocycle scaffolds. *Eur. J. Org. Chem.* **2014**, *34*, 7614-7620.

(28) De Marco, R.; Mazzotti, G.; Dattoli, S. D.; Baiula, M.; Spampinato, S.; Greco, A.; Gentilucci, L. 5-Aminomethylloxazolidine-2,4-dione hybrid  $\alpha/\beta$ -dipeptide scaffolds as inductors of constrained conformations: applications to the synthesis of integrin antagonists. *Biopolymers* **2015**, *104*, 636-649.

(29) Bedini, A.; Baiula, M.; Gentilucci, L.; Tolomelli, A.; De Marco, R.; Spampinato, S. Peripheral antinociceptive effects of the cyclic endomorphin-1 analog c[YpwFG] in a mouse visceral pain model. *Peptides* **2010**, *31*, 2135-2140.

(30) Liu, H.; Zhang, B.; Liu, X.; Wang, C.; Ni, J.; Wang, R. Endomorphin 1 analogs with enhanced metabolic stability and systemic analgesic activity: design, synthesis, and pharmacological characterization. *Bioorg. Med. Chem.* **2007**, *15*, 1694-1702.

(31) Kivell, B.; Priszczano, T. E. Kappa opioids and the modulation of pain. *Psychopharmacology* **2010**, *210*, 109-119

(32) Butelman, E. R.; Yuferov, V.; Kreek, M.J.  $\kappa$ -opioid receptor/dynorphin system: genetic and pharmacotherapeutic implications for addiction. *Trends Neurosci.* **2012**, *35*, 587-596.

(33) Paton, K. F.; Kumar, N.; Crowley, R. S.; Harper, J. L.; Priszczano, T. E.; Kivell, B. M. The analgesic and anti-inflammatory effects of Salvinorin A analogue  $\beta$ -tetrahydropyran Salvinorin B in mice. *Eur. J. Pain* **2017**, *21*, 1039-1050.

(34) Bidlack, J. M.; McLaughlin, J. P.; Wentland, M. P. Partial

opioids. medications for the treatment of pain and drug abuse. *Ann. N. Y. Acad. Sci.* **2000**, *909*, 1-11

(35) Carlezon, W. A. Jr.; Béguin, C.; Knoll, A. T.; Cohen, B. M. Kappa-opioid ligands in the study and treatment of mood disorders. *Pharmacol. Ther.* **2009**, *123*, 334-343.

(36) Mann, K.; Torup, L.; Sørensen, P.; Gual, A.; Swift, R.; Walker, B.; van den Brink, W. Nalmefene for the management of alcohol dependence: review on its pharmacology, mechanism of action and meta-analysis on its clinical efficacy. *Eur. Neuropsychopharmacol.* **2016**, *26*, 1941-1949.

(37) Aldrich, J. V.; Patkar, K. A.; McLaughlin, J. P. Zyklophin, a systemically active selective kappa opioid receptor peptide antagonist with short duration of action. *Proc. Natl. Acad. Sci. USA* **2009**, *106*, 18396-18401.

(38) Urbano, M.; Guerrero, M.; Rosen, H.; Roberts, E. Antagonists of the kappa opioid receptor. *Bioorg. Med. Chem. Lett.* **2014**, *24*, 2021-2032.

(39) Temussi, P. A.; Picone, D.; Saviano, G.; Amodeo, P.; Motta, A.; Tancredi, T.; Salvadori, S.; Tomatis, R. Conformational analysis of an opioid peptide in solvent media that mimic cytoplasm viscosity. *Biopolymers* **1992**, *32*, 367-372.

(40) Borics, A.; Tóth, G. Structural comparison of mu-opioid receptor selective peptides confirmed four parameters of bioactivity. *J. Mol. Graphics Modell.* **2010**, *28*, 495-505.

(41) Che, T.; Majumdar, S.; Zaidi, S. A.; Ondachi, P.; McCorvy, J. D.; Wang, S.; Mosier, P. D.; Uprety, R.; Vardy, E.; Krumm, B. E.; Han, G. W.; Lee, M. Y.; Pardon, E.; Steyaert, J.; Huang, X. P.; Strachan, R. T.; Tribo, A. R.; Pasternak, G. W.; Carroll, F. I.; Stevens, R. C.; Cherezov, V.; Katritch, V.; Wacker, D.; Roth, B. L. Structure of the nanobody-stabilized active state of the kappa opioid receptor. *Cell* **2018**, *172*, 55-67.

(42) Wu, H.; Wacker, D.; Mileni, M.; Katritch, V.; Han, G. W.; Vardy, E.; Liu, W.; Thompson, A. A.; Huang, X.-P.; Carroll, F. I.; Mascarella, S. W.; Westkaemper, R. B.; Mosier, P. D.; Roth, B. L.; Cherezov, V.; Stevens, R. C. Structure of the human  $\kappa$ -opioid receptor in complex with JD1c. *Nature* **2012**, *485*, 327-332.

(43) Vardy, E.; Mosier, P. D.; Frankowski, K. J.; Wu, H.; Katritch, V.; Westkaemper, R. B.; Aubé, J.; Stevens, R. C.; Roth, B. L. Chemotype-selective modes of action of  $\kappa$ -opioid receptor agonists. *J. Biol. Chem.* **2013**, *288*, 34470-34483.

(44) O'Connor, C.; White, K.L.; Doncescu, N.; Didenko, T.; Roth, B.L.; Czaplicki, G.; Stevens, R. C.; Wüthrich, K.; Milon, A. NMR structure and dynamics of the agonist dynorphin peptide bound to the human kappa opioid receptor. *Proc. Natl. Acad. Sci. USA*, **2015**, *112*, 11852-11857.

(45) Brust, A.; Croker, D. E.; Colless, B.; Ragnarsson, L.; Andersson, Å.; Jain, K.; Garcia-Caraballo, S.; Castro, J.; Brierley, S. M.; Alewood, P. F.; Lewis, R. J. Conopeptide-derived  $\kappa$  opioid agonists (Conorphins): potent, selective, and metabolically stable dynorphin A mimetics with antinociceptive properties. *J. Med. Chem.* **2016**, *59*, 2381-2395.

(46) Przydział, M. J.; Pogozheva, I. D.; Bosse, K. E.; Andrews, S. M.; Tharp, T. A.; Traynor, J. R.; Mosberg, H. I. Roles of residues 3 and 4 in cyclic tetrapeptide ligand recognition by the kappa-opioid receptor. *J. Pept. Res.* **2005**, *65*, 333-342.

# Table of Contents

